Linking Land use/Cover and Fossil Energy Consumption to Detect the Carbon Footprint Changes in the Yangtze River Delta, China

Yan Xia and Fengsong Pei*

School of Geography, Geomatics and Planning, Jiangsu Normal University, Xuzhou, 221116, PR China

Abstract: Fossil energy consumption is considered as an important source of carbon emission worldwide. As one of ecological footprint methodology, carbon footprint is emerging as an effective tool for carbon emission management, especially that from fossil energy consumption. Taking one of the most developed regions in China, the Yangtze River Delta as a case study, this paper analyzes carbon footprint of fossil energy consumption through productive lands by explicitly addressing spatial changes of land use/cover. The impacts of land use change on the carbon footprint are then assessed by coupling changes in land use/cover and fossil energy consumption. The results show that carbon footprint from energy consumption in the Yangtze River Delta increased from 322531 km^2 in 2001 to 862924 km^2 in 2013. Despite the fact that productive lands (*i.e*., forest and grasslands) were rising, the carbon footprint was still in deficit, about 831873 km^2 in 2013. According to scenario analysis, carbon footprint is expected to reach 2572837 km^2 in 2025 in the condition of ecological protection, 2604049 km^2 in the condition of business as usual and 2609125 km^2 in cultivated land protection. The results propose urgent policy measures to protect productive lands to reduce the ecological pressure of carbon emissions from energy consumption.

Keywords: Fossil energy consumption, Carbon footprint, Productive lands, GeoSOS-FLUS.

1. INTRODUCTION

The global land surface temperature increased rapidly, at a rate of 1.59 °C between 1850 and 1900 and between 2011 and 2020 (IPCC, 2021). The warming is likely to be mainly due to continuously increase in fossil energy consumption and therefore its carbon emission (Oreskes, 2004). The carbon emission from fossil energy consumption is widely concerned by scientific communities in recent years. Luderer *et al*. (2018) explored the residual carbon dioxide (CO_2) emissions from fossil fuels to hold global warming in 1.5–2 °C pathways to reach the goals of the Paris Agreement. McGlade and Ekins explored the emissions limit for fossil fuel production to limit global warming to 2 °C in different regions (Christophe and Paul, 2015). Despite widespread concerns, few researches addressed the carbon emission from aspects of carbon accumulation by terrestrial ecosystems to offset it (Piao *et al*., 2009; Tigges and Lakes, 2017).

Ecological footprint tracks national economies energy and resource throughput and translates them into biologically productive areas necessary to produce these flows (Inch, 1995; Wackernagel *et al*., 1999; Fang *et al*., 2014). As one of ecological footprint, carbon footprint (CF) refers to the land area to assimilate the CO_2 produced by the mankind (Pandey *et al*., 2011). In recent years, carbon footprint becomes one of the widely recognized methods to evaluate the impacts of carbon emissions on the environment pressure (Fantozzi and Bartocci, 2016). For instances, Simion *et al*. (2013) proposed an ecological footprint indicator by integrating land occupation, CO_2 emissions from fossil energy and nuclear energy use to do environmental sustainability assessment in European countries. Zhao *et al*. (2014) estimated the carbon emissions and carbon footprint in Nanjing city from 2000 to 2009. Ma *et al*. (2018) analyzed the ecological pressure of carbon footprint in passenger transport for all the provinces and autonomous regions of China over the period 2006–2015. Chuai *et al*. (2012) assessed the carbon emission from energy consumption and carbon footprint in different regions of China from 1999 to 2008. Qian *et al*. (2015) analyzed the land carrying capacity using ecological footprint and index system method by using Xiamen City, China as a case. Although many studies addressed such issue as carbon footprint of energy use, few works addressed the effects of land use/cover changes and thus productive land changes on it. Therefore, more attention should be paid to the relationships between carbon footprint and land use/cover changes (Jeroen and Grazi, 2014).

This paper examines temporal-spatial changes of land use/cover on carbon footprint by addressing dynamics of productive lands. As one of the bottom-up approaches, Cellular Automata (CA) has been widely employed in simulating spatial dynamics of land cover/use change (Clarke *et al*., 1997; Wu and Webster, 1998; Xia *et al*., 2013). In particular,

*Address correspondence to this author at the School of Geography, Geomatics and Planning, Jiangsu Normal University, No.101 Shanghai Road, Tongshan New District, Xuzhou 221116, P.R. China; Tel: (+86)15162226524; E-mail: fengsong.pei.jsnu@gmail.com; peifs@jsnu.edu.cn

E-ISSN: 2311-8741/22

GeoSOS-FLUS which was developed from CA, has advantages on explicitly simulating long-term spatial trajectories of multiple land use/cover changes (Liu *et al*., 2017). In addition, Markov chain model has a merit on describing the probabilistic relationship between the attributes of a variable and the position of this variable in a time sequence, including land use change (Bourne, 1969). On this basis, carbon footprint model is to be improved by explicitly addressing spatial changes of land use/cover. To reflect probable changes in land use/cover change, scenario analysis was performed assuming future developments of ecological protection, business-as-usual and cultivated land protection. As one of the most developed and densely populated regions in China, the Yangtze River Delta (YRD) was selected as a case study. The objectives of this study were to (1) analyze the land use/cover change by coupling Markov and GeoSOS-FLUS, (2) propose an improved carbon footprint model by explicitly addressing spatial changes of land use/cover, and (3) detect the carbon footprint changes by linking land use/cover and fossil energy consumption using the Yangtze River Delta, China as an instance.

2. STUDY AREA AND DATA PREPROCESSING

2.1. Study Area

In this paper, the study area is located in the Yangtze River Delta (YRD) (Figure **1**). The YRD lies between 118°E–123°E and 28°N–34°N, with an area of 104,985 km^2. As one of sub-tropical monsoon region, the YRD is known as its favorable conditions including concurrent rainfall and heat energy on vegetation growth. Furthermore, it encompasses the entire city of Shanghai, the southern part of Jiangsu Province (Suzhou, Wuxi, Changzhou, Nanjing, Zhenjiang, Nantong, Taizhou, Yangzhou) and the northern part of Zhejiang Province (Hangzhou, Ningbo, Shaoxing, Jiaxing, Huzhou, Taizhou and Zhoushan). Since economic reform in China in 1978, the YRD has witnessed fast industrialization and unprecedented urbanization. The gross domestic product (GDP) in the YRD reached US$ 3.06 trillion in 2021 (approximately 17.26% of the total GDP in China).

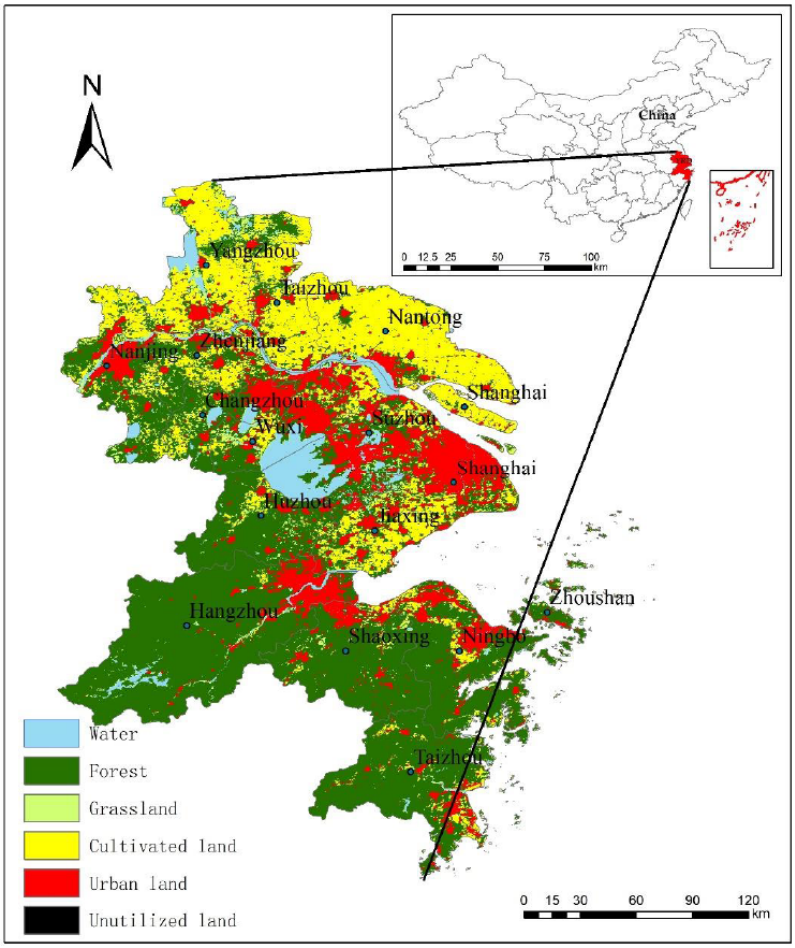

Figure 1: The location of Yangtze River Delta.

2.2. Data and Preprocessing

The data in this study includes time series of data on fossil energy consumption in the aforementioned 16 cities, land use data, net primary productivity data (NPP), digital elevation model (DEM) data, transportation and administrative boundaries data. The fossil energy consumption data were collected for the period 2001-2013 from several statistical yearbooks, including China's energy statistical yearbook, statistical yearbook of Jiangsu Province, statistical yearbook of the YRD, statistical yearbooks of Taizhou and Zhoushan. For assuring continuity and consistency, raw coal, gasoline, diesel and electric power were selected from 2001 to 2013. As to the land use and the NPP data, the Moderate Resolution Imaging Spectroradiometer (MODIS) products (MCD 12 and MOD17A3) was downloaded from NASA's Land Processes Distributed Active Archive Center (LP DAAC). The original data were projected from their original sinusoidal projection to geographic grid cells using MODIS Reprojection Tool (MRT). Locational (spatial) factors including various proximities to attraction centres were addressed to drive land use changes (Liu *et al*., 2017). All the spatial proximities variables were obtained using Geographic Information System (GIS).

3. METHODS

3.1. Coupling Markov and GeoSOS-FLUS to Simulate Land use Change

In past decades, many methods were proposed to capture land use/cover changes, including non-spatial and spatial models (Huang and Cai, 2017). In this paper, temporal-spatial dynamics of the land use/cover were modeled by coupling the Markov and GeoSOS-FLUS. In detail, the amount of various land use/cover was first modeled using the first-order Markov model (Bourne, 1969). Taking the land use/cover area in 2000 as the initial state matrix: $S_{init} = [S_1, S_2, S_3, S_4, S_5, S_6,]$, transfer matrix of various land use type from 2000 to 2013 can be obtained as follows:

$$P_{ij}(n) = \begin{bmatrix} P_{11} & P_{12} & \cdots & P_{1n} \\ P_{21} & P_{22} & \cdots & P_{2n} \\ \cdots & \cdots & \cdots & \cdots \\ P_{n1} & P_{n2} & \cdots & P_{nn} \end{bmatrix} \quad (1)$$

where $0 \le P_{ij} \le 1$ 且 $\sum_{j=1}^{n} P_{ij} = 1$. The state after transferred (S_{trans}) for *m* times can therefore be obtained as:

$$S_{trans} = S_{init} \times p_{ij}(n)^m \quad (2)$$

Based on the results from Markov prediction, spatial pattern of the land use/cover was simulated using GeoSOS-FLUS. The GeoSOS-FLUS was firstly developed by coupling system dynamics (SD), artificial neural network (ANN) and geographical cellular automata. It is an integrated model for multi-type land use scenario simulations by coupling human and natural effects (Liu *et al*., 2017). Firstly, ANN is used to train and estimate the probability-of-occurrence of each land use type on a specific grid cell. In the input layer, input variables include distance-based and natural variables can be mathematically expressed as:

$$X = \begin{bmatrix} x_1 & x_2 & \cdots & x_n \end{bmatrix}^T \quad (3)$$

where x represents the slope, distances to city center, railway, highway, roadway, forest, grassland and so on. In the hidden layer, the signal received from all the input neurons on grid cell *p* at time *t* is estimated as:

$$net_j(p,t) = \sum_i wij \times x_i(p,t) \quad (4)$$

where W_{ij} means an adaptive weight between the input layer and the hidden layer, which is calibrated in the training process. Further, the probability-of-occurrence P(p,k,t) of land use type k on grid cell p at training time *t* is estimated according to the following equation:

$$p(p,k,t) = \sum_j w_{j,k} \times sigmoid(net_j(p,t)) = \sum_j w_{j,k} \frac{1}{1+e^{-net_j(p,t)}} \quad (5)$$

where $w_{j,k}$ is an adaptive weight between the hidden layer and the output layer. To reflect the represent the inheritance of previous land use types among different land use types, inertia coefficient is defined as:

$$Inertia_k^t = \begin{cases} Inertia_k^{t-1} & if \left|D_k^{t-2}\right| \le \left|D_k^{t-1}\right| \\ Inertia_k^{t-1} \times \dfrac{D_k^{t-2}}{D_k^{t-1}} & if\, 0 > D_k^{t-2} > D_k^{t-1} \\ Inertia_k^{t-1} \times \dfrac{D_k^{t-1}}{D_k^{t-2}} & if D_k^{t-1} > D_k^{t-2} > 0 \end{cases} \quad (6)$$

where D_k^{t-1} denotes the difference between the macro demand and the allocated amount of land use type k until iteration time t-1.

By coupling Markov and GeoSOS-FLUS, land use/cover change in the YRD was simulated under

three different scenarios: business as usual (BAU), urban development and ecological protection (UEP), and urban development and cultivated land protection (UCP).

3.2. IPCC Carbon Inventory and Grey Model Methods to Estimate Carbon Emission from Fossil Energy Consumption

There are many ways to estimate carbon emissions, including life cycle assessment (LCA), input output method (IO), Kaya carbon emission identity method and IPCC carbon inventory method (IPCC, 1996; Mahony, 2013; Jing *et al*., 2016; Jiang and Li, 2017). In this paper, carbon emissions from fossil energy consumption was calculated using carbon inventory method recommended by IPCC. For the i-*th* energy (E_i, ton), its carbon emission (E_i) could be calculated as:

$$E_i = M_i \times F_i \quad (7)$$

where M_i is the total amount of i-th type of energy consumption (10^4 tce); F_i is the carbon emission coefficient of the i-th energy (t C tce^{-1}). Table **1** shows the standard coal coefficient and carbon emission coefficient of raw coal, gasoline and diesel.

Table 1: Carbon Emission Factor for Different Types of Fuels

Types	Standard Coal Coefficient	Carbon Emission Coefficient
Raw coal	0.7143 (kgce/kg)	0.7559(10^4t/10^4tce)
Gasoline	1.4714 (kgce/kg)	0.5538(10^4t/10^4tce)
Diesel	1.4571 (kgce/kg)	0.5921(10^4t/10^4tce)

Based on equation 7, carbon emission from raw coal, gasoline and diesel was calculated for the period 2001-2013. Furthermore, Grey Model was employed to estimate future carbon emission. Concretely, a grey system refers to a system with the fuzziness of hierarchical and structural relations, the randomness of dynamic changes, and the incomplete or indeterminacy of the index data (Deng, 1990). In particular, Grey Model was widely employed in forecasting energy consumption and carbon emission (Boran, 2015; Hamzacebi and Karakurt, 2015; Fei *et al*., 2015).

As one of important components of grey system theory, Grey Model is characterized by simple modeling process, concise model expression, easy solution and wide application (Hsu *et al*., 2003; Lee and Tong, 2011). In particular, GM(1,1) model, which consists of a first order differential equation containing only one variable, is the most commonly applied grey model (Dai *et al*., 2018; Wang *et al*., 2018). In this paper, the GM (1, 1) was employed to estimate the carbon emissions assuming a continually consistent development of economy, population and technological innovation in present periods. If $X^{(0)} = (x^{(0)}(1), x^{(0)}(2), \ldots, x^{0}(n))$ is an original sequence with non-negative values, the GM (1,1) can be established as follows:

Conduct an accumulated generating operation of x(0) to obtain sequence x(1):

$$x^{(1)} = \left[x^{(1)}(1), x^{(1)}(2), \cdots, x^{(1)}(n)\right] \quad (8)$$

where the accumulated generating operator (AGO) is defined as $x^{(1)}(k) = \sum_{i=1}^{k} x^{0}(i)$ (k=1, 2, …, n). Furthermore, $x^{(1)}(k)$ satisfies the following first order linear differential equation model:

$$\frac{dx^{(1)}}{dt} + ax^{(1)} = u \quad (9)$$

$$[a, u]^T = (B^T B)^{-1} B^T Y_N \quad (10)$$

where:

$$B = \begin{bmatrix} -\frac{1}{2}\left[x^{(1)}(1) + x^{(1)}(2)\right] & 1 \\ -\frac{1}{2}\left[x^{(1)}(2) + x^{(1)}(3)\right] & 1 \\ \cdots & \cdots \\ -\frac{1}{2}\left[x^{(1)}(n-1) + x^{(1)}(n)\right] & 1 \end{bmatrix} \quad (11)$$

$$Y_N = \begin{bmatrix} x^{(0)}(2) \\ x^{(0)}(3) \\ \cdots \\ x^{(0)}(\mathrm{n}) \end{bmatrix} \quad (12)$$

Based on equation 9, x(1)(t + 1) can be solved as:

$$\hat{x}^{(1)}(k+1) = \left(x^{(0)}(1) - \frac{u}{a}\right)e^{(-ak)} + \frac{u}{a}(k = 1,2,\cdots,n) \quad (13)$$

Finally, the inverse AGO method is employed to obtain the forecasting value:

$$\hat{x}^{(0)}(k+1) = \hat{x}^{(1)}(k+1) - \hat{x}^{(1)}(k)(k = 1,2,\cdots,n) \quad (14)$$

Further details about the GM (1, 1) can be found in Deng's and Wang's studies (Jiang and Li, 2017; Wang *et al*., 2018).

3.3. Assessing the Changes of Carbon Footprint in the YRD

In this paper, carbon emission of fossil energy consumption from 2001 to 2013 was estimated using IPCC carbon inventory. Probable changes of the carbon emission were further predicted using the GM(1,1) model. By using the NPP as an indicator of carbon absorption, carbon deficits were analyzed between carbon absorption and carbon emission from fossil energy consumption. In addition, carbon footprint of fossil energy consumption was calculated using an improved method by explicitly addressing spatial changes of land use/cover. The carbon footprint deficits were then analyzed by comparing existing productive land area with the carbon footprint from fossil energy consumption.

Past studies found that forest and grassland show mainly carbon sequestration effect. However, cultivated land and urban land are frequently carbon sources (Fang *et al*., 2007; Pei *et al*., 2018; Pei *et al*., 2021). Assuming forest and grassland as productive lands, carbon footprint was calculated as: (1) analyze the carbon absorption of forest and grassland based on published literatures; (2) calculate the carbon absorption ratio of the YRD according to the average carbon absorption coefficient and the land area; (3) analyze the productive land area to absorb carbon emissions from fossil energy consumption. In this paper, an improved carbon footprint model was proposed to address spatial changes of land use/cover. That is, the proportion of the forest and grassland is simulated to reflect the effect of land use/cover changes on carbon footprint. In detail, the carbon footprint of fossil energy is calculated as follows:

$$A_{reg} = \sum_i^4 \frac{C_i \times F_i \times P_{erf}}{EP_f} + \frac{C_i \times F_i \times P_{erg}}{EP_g} \quad (15)$$

where A_{reg} is the total amount of carbon footprint of fossil energy consumption (hm^2) of the i-th region; C_i is the i-th type of fossil energy consumption (1×10^4tce), where the energy is raw coal, gasoline and diesel; F_i is the carbon emission coefficient of the i-th energy (tC tce^{-1}); EP_f and EP_g is the net ecosystem production (NEP) of the forest and grassland, respectively; In this study, the EP_f and EP_g was determined as global average NEP of the corresponding vegetation type (*i.e*., 3.809592 tC hm^{-2} for forest and 0.948229 tC hm^{-2} for grassland) (Xie *et al*., 2008; Chen *et al*., 2013); P_{erf} and P_{erg} are the carbon absorption ratios of forest and grasslands in the YRD respectively. In past studies, the terms; P_{erf} and P_{erg} was frequently calculated using quantitative analysis. In particular, productive lands (forests, grasslands, arable lands, gardens, and other agricultural lands) contain different carbon stock due to difference of the land use/covers locally. It is difficult to reflect the effect of temporal-spatial pattern of various land use/covers on them using such method. Thus, land use/cover change and the NPP were introduced to reflect the impacts of spatial changes of land use/cover on carbon footprint. The ratio of the forest and grassland was calculated to estimate the productive land as follows:

$$P_{erf} = \frac{Absp_f}{Absp_f + Absp_g} \quad (16)$$

where P_{erf} is the forest absorption ratio; $Absp_{fi}$ is the absorption of the forestland; $Absp_g$ is the absorption of the grassland. Both the and $Absp_g$ were compiled using the NPP dataset from MODIS products. The absorption ratio of grassland is calculated in the same way as forest lands.

4. RESULTS

4.1. Validation of the GeoSOS-FLUS and GM (1,1)

In this study, a cell-by-cell comparison was conducted to validate the GeoSOS-FLUS model when

Table 2: Confusion Matrix and Kappa Coefficient between Actual and Simulated Land use in the YRD

Actual	Simulated						
	Water	Forest	Grass land	Cultivated lands	Urban lands	Unused lands	Accuracy%
Water	2379	0	3	0	0	0	99.87
Forest	4	20397	586	1432	924	5	87.36
grassland	4	388	395	235	80	12	35.46
Cultivated lands	0	1838	63	7444	286	2	77.28
Urban lands	0	857	13	499	5450	4	80.47
Unused lands	0	2	12	0	3	17	50
Kappa	0.74						

simulating the land use change in the YRD. We further analyzed confusion matrix and kappa coefficient of the simulated land use in the YRD in 2013 (Table **2**). We found that the Kappa coefficient is 0.774. The results suggest that the GeoSOS-FLUS model can be effective in simulating the land use change in the YRD. In addition, the GM (1,1) was validated using time series of carbon emission records in the YRD from 2001 to 2013. As shown in Figure **2**, a good accordance could be found between the simulated values and the measured carbon emission (R=0.93; N=208; P=0.000).

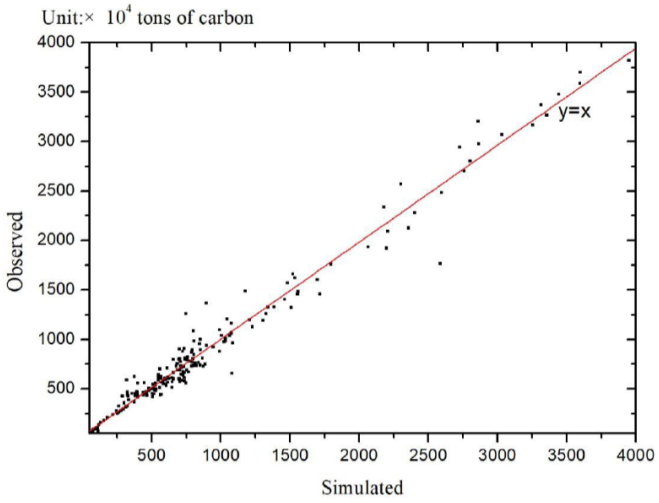

Figure 2: Comparison of actual and simulated carbon emission.

4.2. Changes of Land use/Cover in the YRD

As shown in Figure **3a**, land use/cover types in the YRD is mainly forest and cultivated lands. The proportion of forest, cultivated lands, grassland and urban lands in 2001 in the YRD is 56%, 26%, 2% and 11%, respectively. With the fast urbanization, large cultivated lands were replaced into urban land use. For instances, the cultivated lands showed an obvious decrease, approximately 22% of the YRD in 2013 (Figure **3b**). The proportion of urban lands increased to about 16% of the whole region in 2013, instead. The forest lands firstly showed an increased trend before 2008, and then declined owing to the project and policies about conversing cropland to forest or grass lands in China (Liu *et al*., 2017). In addition, grassland showed a small increase in past decade. Future land use was further analyzed for the period 2014-2025 by assuming different development strategies, including BAU, UEP and UCP scenarios. We found that forest and cultivated lands are to be reduced in the process of rapid urban expansion in the BAU scenario in the YRD. As to the productive land area in the BAU, UEP and UCP scenarios, we found that the changes in productive land area is similar in that of forest land area. In detail, the productive land area showed an increasing trend before 2008, at a rate of 268 km^2 $year^1$. However, such trends were reversed in 2008. Despite the increase of grassland, total productive land

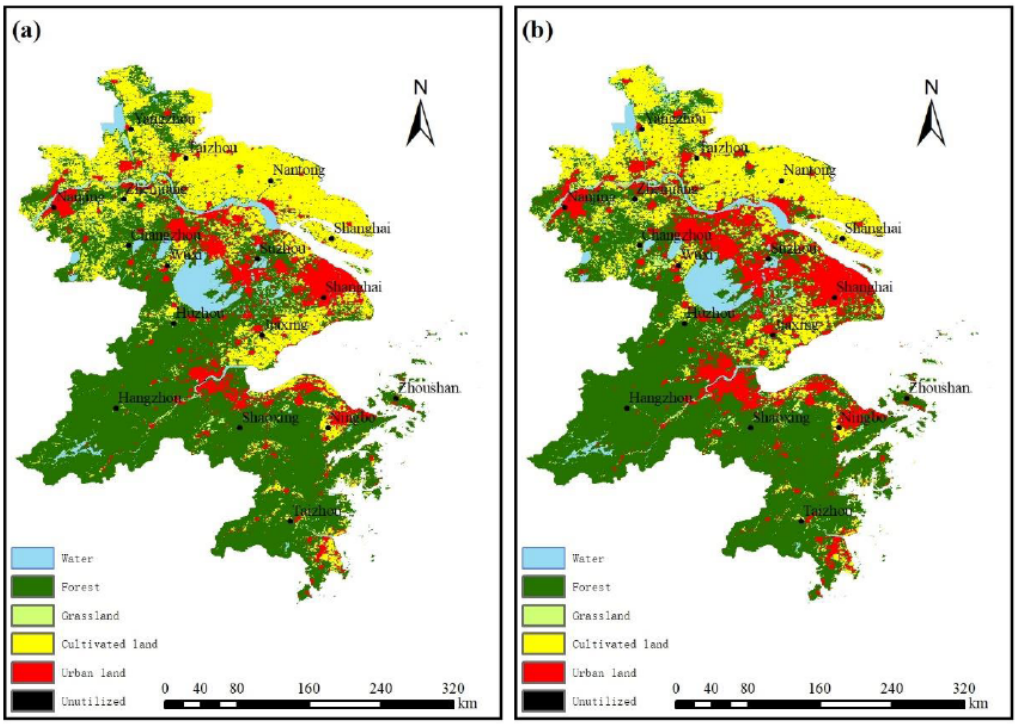

Figure 3: Spatial distributions of the land use for the years 2001 and 2013.

area still showed a decrease, at a rate of 27 km^2 $year^{-1}$ in the UEP scenario, 250 km^2 $year^{-1}$ in the BAU scenario and 425 km^2 $year^{-1}$ in the UCP scenario, respectively.

4.3. Changes of Carbon Emission and Absorption

Both carbon emission and carbon absorption were analyzed in the YRD over the period from 2001-2025. In particular, carbon emissions from fossil energy consumption were increasing in the YRD from 2001 to 2013, at a rate of 986.83×10^4 tons $year^{-1}$ (R^2=0.943; P=0.000). Assumed that no technology and policy reformation, the carbon emissions in the YRD are expected to rise up to nearly 500 million tons of carbon in 2025, approximately 6 times more than that in 2001.

To examine changes of the carbon deficit in the YRD, the carbon absorption by terrestrial ecosystems was also analyzed from 2001 to 2025. According to our calculations, average carbon absorption from 2001 to 2013 was 2307.40×10^4 tons. In particular, the carbon absorption reached 2354.68×10^4 tons of carbon in 2008, probably due to the project and policies about conversing cropland to forest or grass lands in China (Liu *et al.*, 2017). In addition, average carbon absorption reached 2186.96×10^4 tons of carbon over the period 2014-2025 in the BAU scenario. However, average carbon absorption reached 2232.99×10^4 tons of carbon and 2153.17×10^4 tons of carbon in the UEP and UCP scenarios, respectively.

We further analyzed changes of the carbon deficits between carbon emission from energy consumption and the carbon absorption by terrestrial ecosystems in the YRD. We found that carbon deficits in the YRD showed an overall increasing trend over the period 2001-2025, at a rate of 1560.1 tons of carbon·$year^{-1}$ to 1566.1 tons of carbon·$year^{-1}$ owing to different development strategies in future decade. However, an obvious difference in the carbon deficits could be found between 2001-2013 and 2014-2025. In the period 2001-2013, the carbon deficit ranged between 6069.88×10^4 tons of carbon in 2001 and 317482.79×10^4 tons of carbon in 2013. From 2014 to 2025, the carbon deficit could be different under the aforementioned three scenarios in the YRD. Concretely, carbon deficit can reach 47251.68×10^4 tons of carbon, 47168.96×10^4 tons of carbon and 47312.32×10^4 tons of carbon by 2025 in the BAU, UEP and UCP scenarios, respectively. The carbon deficit is expected to strengthen in the condition of similar energy technology in future decades.

In addition, spatial heterogeneities of carbon emissions, carbon absorption and its carbon deficit were further analyzed by cities for the periods 2001-2013 and 2014-2025, respectively. Figures **4a** and **4b** show annual average carbon emissions in the YRD

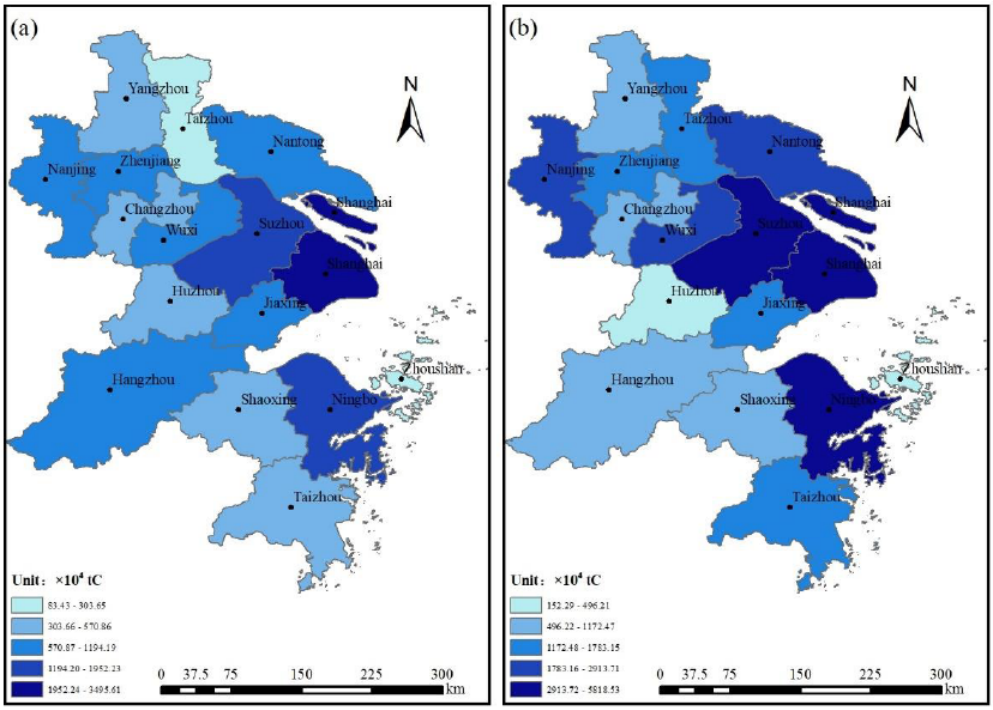

Figure 4: Spatial distribution of average carbon emission for the period (**a**) 2001-2013 and (**b**) 2014-2025.

over the period 2001-2013 and 2014-2025, respectively. Overall, the cities in the eastern YRD consumed more fossil energy and thus produced more carbon emission than other regions in the period 2001-2013 (Figure **4a**). The carbon emission was particularly high in Shanghai, approximately 35 million tons of carbon. In addition, the carbon emissions were relatively lower in Suzhou and Ningbo than in Shanghai. In contrary, Zhoushan had the least carbon emission, about 0.83 million tons of carbon. Figure **4b** shows the predicted average carbon emissions from fossil energy consumption by cities from 2014 to 2025. We found that all cities show obvious increases in the carbon emissions between 2014 and 2025 in the YRD. However, the distribution of carbon emission is overall similar to that of average carbon emissions from 2001 to 2013. That is, cities with large carbon emission are mainly distributed in the eastern YRD, including Suzhou, Shanghai and Ningbo. In particular carbon emission in Suzhou City is expected to show the fastest increase of the carbon emission in the YRD (3.13 million tons of carbon per year). In addition, Zhoushan can still exhibit the slowest increase in carbon emission among the 16 cities in the study area, at a rate of only 0.06 million tons of carbon per year.

Figure **5a** shows average carbon absorption in the YRD from 2001 to 2013. On the whole, the carbon absorption shows a gradual decreasing trend from southwest to northeast. In particular, the carbon absorption was relatively small in Nantong, Zhoushan, Jiaxing, Shanghai and Taizhou (in Jiangsu Province) (less than 60×10^4 tons of carbon). In contrary, Hangzhou, Taizhou, Shaoxing, Ningbo, Huzhou (in Zhejiang Province), Nanjing and Suzhou have over 100×10^4 tons carbon absorption. Carbon absorption during 2014-2025 was also analyzed based on three different development strategies: BAU, UEP and UCP scenarios. Similar pattern could be found between the three different scenarios and the average carbon absorption during 2001-2013 (Figure **5a**). Nevertheless, some differences could also be found among the three scenarios. For instances, it can have the least carbon absorption in Zhoushan City, approximately 30.11×10^4 tons of carbon in the UEP scenario, 29.86×10^4 tons of carbon in the BAU scenario and 29.51×10^4 tons of carbon in the UCP scenario. In contrary, Hangzhou can have the maximum carbon absorption in the YRD, about 548.17×10^4 tons of carbon in the UEP scenario, 545.26×10^4 tons of carbon in the BAU scenario, 544.02 tons of carbon in the UCP scenario, respectively.

The carbon deficit in the period 2001-2013 was also calculated to estimate the carbon balance in the YRD. As shown in Figure **5b**, the carbon deficit in the middle and eastern part of the YRD was even higher than the cities in other regions. Concretely, carbon deficits in several economically developed cities such as Shanghai, Suzhou, Ningbo and Wuxi were relatively

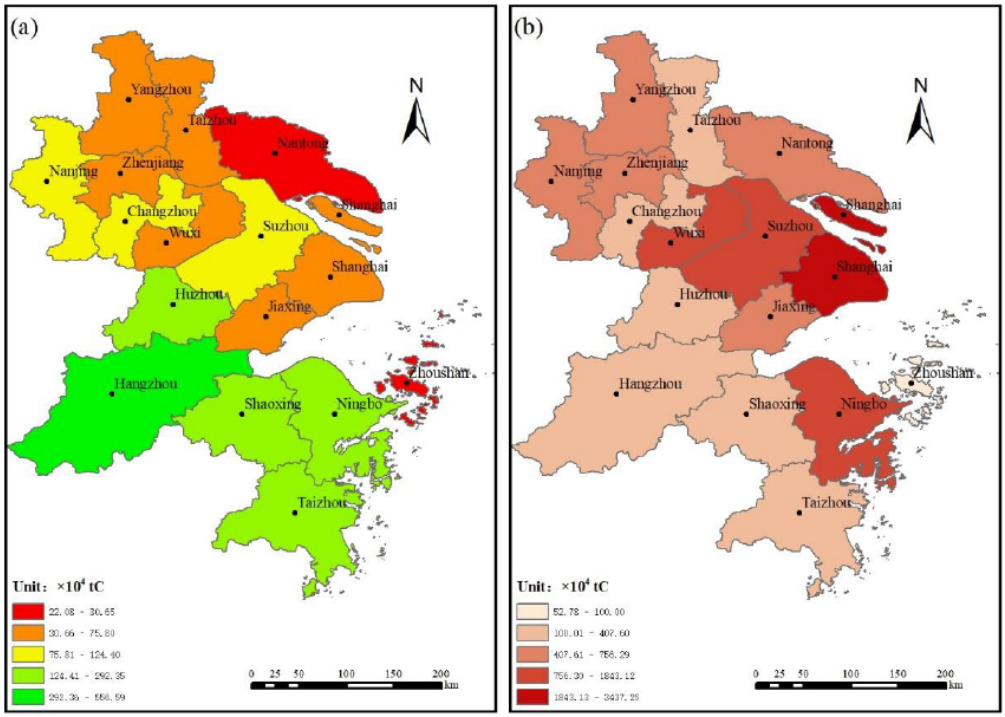

Figure 5: Spatial distributions of (**a**) average carbon absorption and (**b**) carbon deficit from 2001-2013.

large, exceeding 1000×10^4 tons of carbon. In contrary, Zhoushan has the least carbon deficit, about 52.78×10^4 tons of carbon. As to the carbon deficit during 2014-2025, large differences could be found among the 16 cities in the YRD. For instance, average carbon deficit in Suzhou was approximately 47 times as much as that in Zhoushan. In details, the carbon deficit in Zhoushan is 122.18×10^4 tons of carbon in the UEP scenario, 122.43×10^4 tons of carbon in the BAU scenario and 122.78×10^4 tons of carbon in the UCP scenario. In addition, it is 5725.14×10^4 tons of carbon in the UEP scenario, 5731.45×10^4 tons of carbon in the BAU scenario and 5734.10×10^4 tons of carbon in the UCP scenario in Suzhou, respectively. Despite it, similar patterns of the carbon deficit in different cities could also be found between the three scenarios and the average carbon deficits during 2001-2013.

4.4. Changes of Carbon Footprint

We found that the carbon footprint deficit from energy consumption was on the rise in the YRD from 2001 to 2013. Particularly, it reached 468455 km^2 in 2013, about three times as many as that in the year of 2001. Furthermore, the carbon footprint deficit is expected to be continually increased in future. Concretely, the carbon footprint during 2014-2025 could be different in different development strategies. We found that changes in productive lands could reduce the carbon footprint. However, the effects are to be very limited. Carbon footprint is expected to be much more than the actual productive land area during 2014-2025 even if it is in the UEP scenario. That is, it is limited to reduce the carbon footprint from energy consumption by only regulating the land use pattern in the YRD because of the shortage of productive lands. As a result, carbon footprint deficit was and will be rising in the YRD in future. For example, from 2001 to 2013, the carbon footprint was increasing from 229259 km^2 to 547427 km^2 while productive land was decreasing from 81706 km^2 to 79479 km^2. At the same time, carbon footprint deficit was increasing from 148069 km^2 to 468455km^2. The carbon footprint deficit is estimated to be 1296080 km^2 in 2025 even in the UEP scenario.

To further elucidate the difference, changes in carbon footprint, as well as carbon deficits were spatially analyzed by cities in the YRD for the periods 2001-2013 and 2014-2025, respectively. For the period 2001-2013, we found that carbon footprint deficit was more serious in the central and eastern YRD than other parts in the region. In detail, average carbon footprint in Shanghai was approximately 96162km^2, approximately 40 times more than that in Zhoushan, which had the least average annual carbon footprint among the 16 cities in the YRD. Average carbon footprint in Suzhou was up to 53155 km^2, about half of the carbon footprint in Shanghai. In addition, it is obvious that spatial distribution of carbon footprint deficits shares nearly the same principle with that of carbon emission. During 2014-2025, spatial distributions of carbon footprint and deficit will be similar to that during 2001-2013 in all three aforementioned development strategies. In particular, Suzhou is expected to have the highest carbon footprint in the YRD in 2025, with 163877 km^2, 160556 km^2 and 170379 km^2 in the BAU, UEP and UCP scenarios, respectively. In addition, Zhoushan can also have the least carbon footprint and deficit, merely 2.77% of carbon footprint and 2.16% deficit in Suzhou in the UEP scenario.

5. DISCUSSIONS

With fast industrialization and unprecedented urbanization, energy consumption is continuously increasing, and therefore cause large ecological pressures worldwide. In this paper, the impacts of land use change on carbon footprint from fossil energy consumption were assessed using one of typical highly urbanized regions, the YRD in China as a case. To overcome the spatial limit of existing carbon footprint model (Chen *et al*., 2013), an improved carbon footprint model was proposed by explicitly addressing the changes in productive land in the YRD. On this basis, the changes in the carbon footprint were therefore examined by coupling land use changes and carbon emissions from energy consumption. Our results indicate that productive lands could offset and reduce the carbon footprint. However, carbon absorption by terrestrial vegetation was relatively small in comparison with the carbon emission from fossil energy consumption in the YRD. The positive effects of productive lands on carbon emission are to be very limited. Furthermore, the carbon absorption is expected to be reduced according to scenario analysis. The carbon footprint from energy consumption also shows a continuously increasing trend, and are expected to increase in future. Despite the possible postponement by ecological protection, the effect is very limited owing to large fossil energy consumption. Therefore, it is in urgent need to reduce carbon emissions by adjusting the energy structure and strengthening the ecological management (Pei *et al*., 2021).

6. CONCLUSIONS

Taking the Yangtze River Delta, which is one of the most developed regions in China, as a case study, this paper analyzes the carbon footprint of fossil energy consumption using productive lands as an indicator by explicitly addressing spatial changes of land use/cover. The impacts of land use change on the carbon footprint are then assessed by coupling changes in land use/cover and fossil energy consumption. The results propose urgent policy measures to protect productive lands to reduce the ecological pressure of carbon emissions from energy consumption. This paper analyzed the probable changes in future carbon footprint by simulating the energy consumption and land use changes. However, energy consumption is only estimated assuming a continually consistent development of economy, population and technological innovation. Our results may therefore be biased due to limitations of the prediction model. In future studies, we will try to develop different scenarios to reflect economic development and technological advance.

ACKNOWLEDGEMENT

This research was funded by the Qinglan Project of Jiangsu Province in China. The authors also acknowledge the supports on the data processing and original draft from Li-An Liu.

CONFLICTS OF INTEREST

The authors declare no conflict of interest.

REFERENCES

[1] Boran, F. Forecasting natural gas consumption in Turkey using grey prediction. Energy Sources 2015, 208-213. https://doi.org/10.1080/15567249.2014.893040

[2] Bourne, L. Forecasting land occupancy changes through Markovian probability matrices: A central city example. Toronto 1969.

[3] Chen, H.; Li, C., Wang, L. Research on the regional sustainable development based on the ecological footprint theory: a case of Henan Province. Applied Mechanics & Materials 2013, 361-363, 199-203. https://doi.org/10.4028/www.scientific.net/AMM.361-363.199

[4] Christophe, M.; Paul, E. The geographical distribution of fossil fuels unused when limiting global warming to 2°C. NATURE 2015, 517, 187-190. https://doi.org/10.1038/nature14016

[5] Chuai, X.; Huang, X.; Wang, W.; Chen, Z. Temporospatial changes of carbon footprint based on energy consumption in China. J Geogr SCI 2012, 22, 110-124. https://doi.org/10.1007/s11442-012-0915-4

[6] Clarke, K.C.; Hoppen, S.; Gaydos, L. A Self-Modifying Cellular Automaton Model of Historical Urbanization in the San Francisco Bay Area. Environment and Planning B: Planning and Design 1997, 24, 247-261. https://doi.org/10.1068/b240247

[7] Dai, S.; Niu, D.; Han, Y. Forecasting of Energy-Related CO2 Emissions in China Based on GM(1,1) and Least Squares Support Vector Machine Optimized by Modified Shuffled Frog Leaping Algorithm for Sustainability. Sustainability-Basel 2018, 958. https://doi.org/10.3390/su10040958

[8] Deng, J., Application of grey system theory in China, International Symposium on Uncertainty Modeling & Analysis. IEEE, College Park, MD, USA. 1990.1.

[9] Fang, J.; Guo, Z.; Piao, S.; Chen, A. Terrestrial vegetation carbon sinks in China, 1981-2000. Science in China 2007, 50, 1341-1350. https://doi.org/10.1007/s11430-007-0049-1

[10] Fang, K.; Heijungs, R.; Snoo, G.R.D. Theoretical exploration for the combination of the ecological, energy, carbon, and water footprints: Overview of a footprint family. ECOL INDIC 2014, 36, 508-518. https://doi.org/10.1016/j.ecolind.2013.08.017

[11] Fantozzi, F.; Bartocci, P. Carbon Footprint as a Tool to Limit Greenhouse Gas Emissions. 2016. https://doi.org/10.5772/62281

[12] Fei, Y.; Xie, X.; Li, Z.; Hu, X. An Improved Grey Model and Scenario Analysis for Carbon Intensity Forecasting in the Pearl River Delta Region of China. Energies 2018, 11, 91. https://doi.org/10.3390/en11010091

[13] Hamzacebi, C.; Karakurt, I. Forecasting the Energy-related CO2 Emissions of Turkey Using a Grey Prediction Model. Energy Sources 2015, 37, 1023-1031. https://doi.org/10.1080/15567036.2014.978086

[14] Hsu, C.; Chen, C. Applications of improved grey prediction model for power demand forecasting. Energy Conversion & Management 2003, 44, 2241-2249. https://doi.org/10.1016/S0196-8904(02)00248-0

[15] Huang, Q.; Cai, Y. Simulation of land use change using GIS-based stochastic model: the case study of Shiqian County, Southwestern China. Stochastic Environmental Research & Risk Assessment 2007, 21, 419-426. https://doi.org/10.1007/s00477-006-0074-1

[16] Inch, J. Our Ecological Footprint: Reducing Human Impact on the Earth. Population & Environment 1995, 1, 171-174.

[17] IPCC(Intergovernmental Panel on climate Change). Guidelines for National Greenhouse Gas Inventories., London, 1996.

[18] IPCC. Climate Change 2021: The Physical Science Basis. In Contribution of Working Group I to the Sixth Assessment Report of the Intergovernmental Panel on Climate Change; Masson-Delmotte, V., Zhai, P., Pirani, A., Connors, S.L., Péan, C., Berger, S., Caud, N., Chen, Y., Goldfarb, L., Gomis, M.I., *et al.*, Eds.; Cambridge University Press: Cambridge, UK; New York, NY, USA, 2021.

[19] Jeroen, C.; Grazi, F. Ecological Footprint Policy? Land Use as an Environmental Indicator. J Ind Ecol 2014, 18, 10-19. https://doi.org/10.1111/jiec.12045

[20] Jiang, R.; Li, R. Decomposition and Decoupling Analysis of Life-Cycle Carbon Emission in China's Building Sector. Sustainability-Basel 2017, 9, 793. https://doi.org/10.3390/su9050793

[21] Jing, W.; Kai, H.; Yang, S.; Yan, L.; Hu, T.; Yue, Z. Driving forces analysis of energy-related carbon dioxide (CO2) emissions in Beijing: an input-output structural decomposition analysis. J Clean Prod 2016, S1991410843.

[22] Lee, Y.; Tong, L. Forecasting energy consumption using a grey model improved by incorporating genetic programming. Energy Conversion & Management 2011, 52, 147-152. https://doi.org/10.1016/j.enconman.2010.06.053

[23] Liu, X.; Xun, L.; Xia, L.; Xu, X.; Ou, J.; Chen, Y.; Li, S.; Wang, S.; Pei, F. A future land use simulation model (FLUS) for simulating multiple land use scenarios by coupling human and natural effects. Landscape & Urban Planning 2017, 168,

94-116.
https://doi.org/10.1016/j.landurbplan.2017.09.019

[24] Luderer, G.; Vrontisi, Z.; Bertram, C.; Edelenbosch, O.Y.; Pietzcker, R.C.; Rogelj, J.; De Boer, H.S.; Drouet, L.; Emmerling, J.; Fricko, O. *et al*. Residual fossil CO2 emissions in 1.5-2 °C pathways. Nat Clim Change 2018, 8, 626-633.
https://doi.org/10.1038/s41558-018-0198-6

[25] Ma, F.; Wang, W.; Sun, Q.; Liu, F.; Li, X. Ecological pressure of carbon footprint in passenger transport: Spatio-temporal changes and regional disparities. Sustainability-Basel 2018, 10, 317.
https://doi.org/10.3390/su10020317

[26] Mahony, T.O. Decomposition of Ireland's carbon emissions from 1990 to 2010: An extended Kaya identity. Energ Policy 2013, 59, 573-581.
https://doi.org/10.1016/j.enpol.2013.04.013

[27] Oreskes, N. Beyond the ivory tower. The scientific consensus on climate change. SCIENCE 2004, 306, 1686.
https://doi.org/10.1126/science.1103618

[28] Pandey, D.; Agrawal, M.; Pandey, J.S. Carbon footprint: current methods of estimation. Environmental Monitoring & Assessment 2011, 178, 135-160.
https://doi.org/10.1007/s10661-010-1678-y

[29] Pei, F.; Wu, C.; Liu, X.; Xia, L.; Yang, K.; Yi, Z.; Wang, K.; Li, X.; Xia, G. Monitoring the vegetation activity in China using vegetation health indices. Agricultural & Forest Meteorology 2018, 248, 215-227.
https://doi.org/10.1016/j.agrformet.2017.10.001

[30] Pei, F.; Zhong R.; Liu, L.; Qiao, Y. Decoupling the relationships between carbon footprint and economic growth within an urban agglomeration-A case study of the Yangtze River Delta in China. Land 2021. 10(9): 923.
https://doi.org/10.3390/land10090923

[31] Pei, F.; Zhou, Y.; Xia, Y. Application of Normalized Difference Vegetation Index (NDVI) for the Detection of Extreme Precipitation Change. Forests 2021.12(5): 594.
https://doi.org/10.3390/f12050594

[32] Piao, S.; Fang, J.; Ciais, P.; Peylin, P.; Huang, Y.; Sitch, S.; Wang, T. The carbon balance of terrestrial ecosystems in China. Nature 2009, 458, 1009-1013.
https://doi.org/10.1038/nature07944

[33] Simion, I.M.; Ghinea, C.; Maxineasa, S.G.; Taranu, N.; Bonoli, A.; Gavrilescu, M. Ecological footprint applied in the assessment of construction and demolition waste integrated management. Environmental Engineering & Management Journal 2013, 12, 779-788.
https://doi.org/10.30638/eemj.2013.097

[34] Tigges, J.; Lakes, T. High resolution remote sensing for reducing uncertainties in urban forest carbon offset life cycle assessments. Carbon Balance & Management 2017, 12, 17.
https://doi.org/10.1186/s13021-017-0085-x

[35] Qian, Y.; Tang, L.; Qiu, Q.; Xu, T.; Liao, J. A Comparative Analysis on Assessment of Land Carrying Capacity with Ecological Footprint Analysis and Index System Method. Plos One 2015, 10, e130315.
https://doi.org/10.1371/journal.pone.0130315

[36] Wackernagel, M.; Onisto, L.; Bello, P.; Linares, A.C.; Falfán, I.S.L.; GarcíA, J.M.; Guerrero, A.I.S.; Ma, G.S.G. National natural capital accounting with the ecological footprint concept. Ecol Econ 1999, 29, 375-390.
https://doi.org/10.1016/S0921-8009(98)90063-5

[37] Wang, Z.; Li, Q.; Pei, L. A seasonal GM(1,1) model for forecasting the electricity consumption of the primary economic sectors. ENERGY 2018, 154, 522-534.
https://doi.org/10.1016/j.energy.2018.04.155

[38] Wu, F.; Webster, C.J. Simulation of land development through the integration of cellular automata and multicriteria evaluation. Environment and Planning 1998, 103-126.
https://doi.org/10.1068/b250103

[39] Xia, L.; Liu, Y.; Liu, X.; Chen, Y.; Ai, B. Knowledge transfer and adaptation for land-use simulation with a logistic cellular automaton. INT J GEOGR INF SCI 2013, 27, 1829-1848.
https://doi.org/10.1080/13658816.2013.825264

[40] Xie, H.; Chen, X.; Lin, K. The ecological footprint analysis of fossil energy and electricity. Acta Ecologica Sinica 2008, 28, 1729-1735.

[41] Zhao, R.; Huang, X.; Ying, Z.; Ding, M.; Chuai, X. Urban carbon footprint and carbon cycle pressure : The case study of Nanjing. J Geogr Sci 2014, 24, 159-176.
https://doi.org/10.1007/s11442-014-1079-1

Received on 08-11-2022 Accepted on 14-12-2022 Published on 30-12-2022

DOI: https://doi.org/10.12974/2311-8741.2022.10.03